Multi-Tensor Random-Walk Probabilistic Fibre Tracking Algorithms: Solving Complex Fibre Configurations in the Brain

Jeyarasa Pratheepan, Niroji Thayalan

Sri Lanka Institute of Advanced Technological Institute

Abstract - *Object* In this study simple and computationally efficient random-walk probabilistic algorithms are presented for white matter fibre tracking using diffusion MR images. We examine how fibre tracts can be modelled globally by means of random-walk algorithms which capture the uncertainties in local fibre orientations due to noise and partial volume effects.

Materials and Methods Using Monte Carlo methods, the algorithms generate multiple pathways from a single seed location by randomly perturbing the direction of propagation according to the algorithm model at each step. We analyze the random-walk models quantitatively using a synthetic data set and estimate the optimal parameter values of the models. These algorithms are then applied to a multi-tensor model to compute the probabilities of connections between regions with complex fibre configurations. Voxels are classified based on tensor morphologies and a two-tensor model is estimated for planar voxels and a single-tensor model for the remaining voxels. The proposed algorithms are validated and compared to alternative methods on synthetic data, a physical phantom and real-world brain MRI datasets.

Results and Conclusion The results confirm the effectiveness of the proposed approach, which gives comparable results to other probabilistic methods. Our approach is however significantly faster and requires less memory. The results of multi-tensor random-walk algorithms demonstrate that our algorithms can accurately identify fibre bundles in complex fibre regions.

Index Terms - Diffusion Tensor Imaging, Probabilistic Fibre Tracking, Random-Walk, Multitensor, Fibre Crossing

1. INTRODUCTION

The random-walk of water molecules undergoing diffusion is anisotropic in organized tissues such as white matter. Diffusion weighted magnetic resonance imaging (DW-MRI), a non-invasive MRI technique, measures water self-diffusion rates and thus gives an indication of the underlying tissue microstructure. Fibre tractography using DW-MRI allows the study of anatomical connectivity of the brain *in vivo*, and thus there has been much interest in its application to clinical neuro-sciences. For generating fibre-tract trajectories a variety of algorithms have been proposed [1-12], broadly categorized into deterministic or probabilistic techniques.

Deterministic tractography algorithms [1-3] produce only one reconstructed trajectory per seed point, and therefore branching of fasciculi are not represented. Diffusion MRI is inherently a noisy technique, leading to uncertainty associated with each estimate of local fibre orientation. A criticism of deterministic tractography is the lack of measure of confidence or uncertainty of the reconstructed trajectories. A natural way to deal with this problem is to measure uncertainty of the local fibre orientation probabilistically at each voxel. As a result, probabilistic tractography algorithms [4-11] have been developed to determine the connectivity between brain regions and these methods allow branching of white matter tracts as well. Generally, probabilistic algorithms suffer from complex output in the form of a connectivity map and outliers. Recently, we have shown that these limitations can be addressed by computing representative curves to every anatomically distinct region from the seed point using branch-clustering and average curves [12].

Nonparametric probabilistic tracking methods [4-6] are based on bootstrap statistical methods and use as a sampling pool a set of repeated diffusion weighted measurements. Conventional bootstrapping [4] techniques require repeated acquisitions, and therefore scanning times under many clinical circumstances are unacceptable. Model-based bootstrap [5-6] offers an alternative, since it requires only a single data acquisition. However, the methods use large number of tensor volumes and fitting the diffusion tensor for all the volumes is a computationally expensive process. The parametric (model- based) probabilistic algorithms use a distribution of possible propagation directions at each step along the trajectory, with distributions generally defined on the basis of the diffusion tensor model and derived parameters. The uncertainties of the fibre orientations have been modelled in a Bayesian framework by Behrens et al. [7] and Friman et al. [8]. However, the intrinsic drawback of these methods is their computational complexity, since it is necessary to resort to Monte Carlo methods or to evaluate probability density functions (PDF). The methods take more than several hours on a high-end PC [7-8], and this is unacceptable in clinical practice.

Random-walk methods have been used successfully to date in various scientific contexts to estimate the uncertainty statistically. Random-walk probabilistic techniques have previously been applied to the problem of fibre tracking using perturbation methods

by Lazar and Alexander [9] and Prigarin et al. [10]. However, these previous attempts did not utilize the full power of the technique to assess the uncertainty in tractography. Hagmann et al. [11] developed a random-walk model where the fibre distributions are obtained by deflecting a set of directions uniformly distributed onto a sphere using the tensor operator. In this paper three random-walk probabilistic algorithms are developed and implemented to investigate white matter connectivity. The basic concept of these algorithms was originally proposed in a short report by Prigarin et al. [10]. However, the authors did not apply the method to any DW-MR images and they did not exploit the strength of the proposed random-walk models. Here, we combine these random-walk algorithms with tractography and demonstrate for the first time that the methods are qualitatively comparable to other probabilistic methods and computationally faster than them. A thorough quantitative analysis is performed on synthetic data to determine the optimal model parameters.

Conventional DTI tracking approaches have difficulties in brain regions where fibre bundles cross, which may result in a disk-shaped form of the tensor [13]. In such cases, a single diffusion tensor model is no longer valid. The development of new models based on high angular resolution diffusion imaging (HARDI) seeks to provide solutions to this problem [14-17]. The multi-tensor model [14] is a simple generalization of DTI, which replaces the Gaussian model with a mixture of Gaussian densities. Other HARDI approaches have considerable limitations compared to the multi-tensor model [14], such as very long acquisition requirements (e.g. Q-ball imaging [15] and DSI [16]), reliance on the Fourier transform (e.g. DSI [16]) and susceptibility to noise (e.g. spherical deconvolution [17]). The estimation of these models and the tracking processes using them are demanding in terms of memory requirement and processing time (e.g. PASMRI [18]), and are sometimes impractical. Probabilistic tracking methods can be extended to describe higher order diffusion imaging data, for example, Behrens et al. [19] used a mixture of Gaussian models to extend Bayesian DT-based tracking [7], and a model-based bootstrap technique has been used to estimate the uncertainty associated with the Q-ball model by Berman et al. [20].

Building on our preliminary studies [21], two-tensor random-walk probabilistic algorithms are employed that resolve the uncertainty and fibre crossing problems of the common single-tensor fibre tractography methods. The multi-tensor model [14] is only implemented on planar voxels to increase the validity of the algorithms and to decrease the total tensor estimation time. The results from the two-tensor random-walk tractography method are compared to those of commonly used single-tensor and two-tensor deterministic tracking methods on synthetic data with different levels of noise to evaluate the consistency of the tracking methods in a noisy environment and with complex fibre configurations. The performance of the proposed algorithms are measured and compared with existing deterministic and probabilistic algorithms using a physical phantom and healthy human brain data.

Table 1 Three Random-Walk Algorithms.

Algorithm-E	**Algorithm-T**	**Algorithm-TL**
$v_0 = e(D(x_0))$	$v_0 = e(D(x_0))$	$v_0 = e(D(x_0))$
$x_n = x_{n-1} + v_{n-1}\Delta t + \sqrt{\Delta t}\sigma\epsilon_n$	$x_n = x_{n-1} + v_{n-1}\Delta t + \sqrt{\Delta t}\sigma\epsilon_n$	$x_n = x_{n-1} + v_{n-1}\Delta t + \sqrt{\Delta t}\sigma\epsilon_n$
$v_n = e(D(x_n)), (v_{n-1}.v_n) > 0$	$v_n = D(x_n)V_n - 1$	$v_n = c_0 e(D(x_n)) + (1-c_0)((1-c_1)v_{n-1}$
		$\qquad + c_1 D(x_n)v_{n-1}$

2. THEORY

Random-Walk Algorithms: A fibre path can be described as a sequence of three dimensional vectors $x_n \in V$, where n is the discrete step $(0 \le n \le N)$ and V is a bounded set in the 3D Euclidean space, $V \subset R^3$. Fibre tracking algorithms determine how to obtain the sequence of points x_n for a starting point x_0. Let $D(x)$, $x \in V$, be a given tensor field in V and the principal eigenvector of tensor $D(x)$ be denoted by $e(D(x))$.

Deterministic approaches with streamline Euler integration (STE) [1], obtain x_n values following the principal eigenvector. Thus, if the direction of the starting point is $v_0 = e(D(x_0))$ then

$x_n = x_{n-1} + v_{n-1}\Delta t,$ 　　　　(1)

where $v_n = e(D(x_n))$ and Δt is the step size.

An alternative approach, tensor deflection (TEND) [2], for determining tract direction is to use the entire diffusion tensor to deflect the incoming vector (v_{n-1}) direction.

$v_n = D(x_n)v_{n-1}$ 　(2)

The tensor line algorithm (TL), described by Weinstein et al. [3], dynamically modulates the STE and TEND contributions to steer the tract.

$v_n = c_0 e(D(x_n)) + (1-c_0)((1-c_1)v_{n-1} + c_1 D(x_n)v_{n-1})$ (3)

where c_0 and c_1 are user-defined weighting factors that vary between 0 and 1. Note that for $c_0 = 1$, the tensor-line algorithm is equivalent to STE.

Developing on the random-walk models of Prigarin et al. [10] three probabilistic algorithms are presented in this paper, by adding random perturbation to three deterministic differential equations (Table 1). Fibre distributions are obtained by perturbing the major eigenvector of the tensor (Algorithm-E), by deflecting a set of perturbed propagation directions similar to the TEND algorithm (Algorithm-T) or by a combination of STE and TEND (Algorithm-TL). In these algorithms, s_n represents independent standard normal random vectors and $\Delta t, \sigma$ are parameters of the algorithm. A perturbed direction of $e(D(x))$ is obtained by randomly generating normally distributed offsets with mean zero and standard deviation 1. $(v_{n-1}.v_n) > 0$ is an additional constraint to avoid backward jumps.

The step parameter Δt is assumed to be less than 1 and σ defines the intensity of artificial noise added to generate probabilistic tracks. The factor σ controls the degree of variability in tracking. If $\sigma = 0$, then the algorithms become deterministic and the tracks are defined in a unique non-random way.

The weighting factors c_0 and c_1 are user defined ($c_0+c_1=1$) parameters in Algorithm-TL. The algorithm has three directional terms: (i) an STE term weighted by c_0 (ii) a TEND term weighted by $(1-c_0)c_1$ (iii) an undeviated term weighted by $(1-c_0)(1-c_1)$. Estimated trajectories with different properties can be achieved by changing c_0 and c_1.

Since the random-walk algorithms build on the basic deterministic methods (STE, TEND and Tensorline) the results of random-walk algorithms can be influenced by these basic algorithms. For example, in Algorithm-T the incoming vector (v_{n-1}) is multiplied by the diffusion tensor, therefore the tensor deflects the perturbed propagation direction towards the major eigenvector direction while limiting the curvature of the deflection, resulting in smoother tract reconstruction [2].

Fibre Tractography: The probabilistic algorithms described above simulate a macroscopic random walk of a particle through the set of voxels. This random walk is defined by one-to-one jumps where the steps of the jump and its direction are determined by the parameters of the algorithm. In order to map the connectivity of the brain with a single-tensor DTI model, random curves are initiated from seed points and the tracking algorithm then repeats many times from the seed points with the propagation direction randomly varied according to the algorithm.

Probabilistic techniques typically maintain the curvature criterion for the individual streamlines, but relax the anisotropy threshold for stopping trajectories, in order to potentially capture tract information in regions of fibre crossing. The curve elongation therefore stops when the border of the mask is reached or an angle between two consecutive fibre directions greater than a user defined curvature threshold is detected. The connection probability from a seed point to a random voxel within the dataset is defined as the frequency with which streamlines pass through the voxel, normalized for the total number of repetitions. Finally a global connectivity map is estimated, using the connection probabilities between all voxels in the image and the seed point.

3. MATERIALS AND METHODS

3.1 Data Acquisition

Synthetic Data Sets: We used the PISTE data sets [22] (http://cubric.psych.cf.ac.uk/commondti) that were created for the evaluation of tracking algorithms in regions with critical fibre constellations. The tracts were generated by simulating a DTI measurement with 30 diffusion weighted and 4 un-weighted images. The TE in the simulated measurements was 90 ms. A diffusion weighting b factor of 1000 s/mm^2 was chosen. The datasets are $150 \times 150 \times 16$ voxels in size with isotropic voxel side length of 1 mm.

Physical Phantom: We used a common realistic physical phantom dataset [23] with known ground truth (http://www.lnao.fr/spip.php?article157). The images were used as the basis of the 2009 MICCAI Fiber Cup competition. DW-MRI data were acquired on a
3T MRI system with $3 \times 3 \times 3$ mm^3 voxel resolution, b value=1500 s/mm^2 and 65 directions (1 un-weighted and 64 diffusion directions). A single-shot diffusion-weighted twice refocused spin echo EPI pulse sequence was used for data acquisition, while compensating for eddy currents to the first order. The acquisition parameters were field of view FOV=19.2 cm, image size 64 × 64 × 3, repetition time TR=5 s and echo time TE=94 ms providing isotropic resolution.

***In Vivo* Data:** DW-MR images were acquired from three healthy human subjects on a whole-body 1.5 Tesla scanner using a spin-echo EPI pulse sequence with a b-value of 700 s/mm^2 (TE=81 ms, TR=14 s) using 41 diffusion encoding gradients evenly distributed in space and 5 images without any diffusion weightings. Sixty slices were acquired with 2 mm thickness (no gap), which covered the whole brain with 1.875 × 1.875 × 2 mm spatial resolution. DW Images were corrected for eddy current distortion and motion using FSL [24]. The brain was extracted using BET [24]. The DW scan for each subject was registered to the non-DW image of each average, and the non-DW images from each average were registered to the first non-DW image obtained from each subject [25].

3.2 Model Parameter Optimization

Generally, fibre tracking results depend on the use of good-quality diffusion weighted images, together with a suitable algorithm to generate the tracks. However, acquisition of a set of images with sufficiently high quality is time-consuming, and in practice quality is usually compromised to allow shorter scan times. Fibre tractography algorithms may be affected by noise, partial volume effects etc., to varying degrees. The choice of parameters for random-walk algorithms influences the resulting fibre trajectories. The key parameters in random-walk algorithms are the noise ratio σ and step size Δt. It is therefore essential to optimize the parameter values, and determine under which conditions the algorithms can be used.

Synthetic data was analyzed with a single-tensor to estimate the optimal parameters of the random-walk models. Two tensor field geometries were considered: linear (all tensors oriented in parallel) and branching (comprised of an initial linear tract branching into two tracts). Zero-mean Gaussian noise was added (so that the SNR was equal to the average non-DW image intensity divided by the standard deviation of noise [26]) giving a range of SNRs (5-100) for each geometry.

Tracking was performed from six different seed points on two different synthetic models to optimize σ for different levels of SNR. Other parameters such as step size remained constant. For each experiment (geometry, SNR, 3 random-walk algorithms, 6 different seed points), tract estimates were generated for 1000 instances of the noisy diffusion tensor field. The error in tract estimation was analyzed using average minimum distance [12] from the mean curve [12] of generated curves and the ground truth (noise-free data). Average error was reported for each SNR and the three random-walk algorithms.

A similar experiment was used to optimize the number of step sizes (0.05 - 0.5 mm). The performance was evaluated on data with SNR=30 and SNR=15, using the optimized value of σ for each geometry for the three random-walk algorithms from 6 different seed points. The average error was calculated for the three random-walk algorithms.

3.3 Two-Tensor Random-Walk Tractography

Two-Tensor Estimation: The performance of the random-walk algorithms was further considered when two tensors are allowed to cross within a single voxel. The signal attenuation equation for a generalized two-tensor model can be described by a weighted sum of two Gaussian functions [14]:

$$S_i = S_0 f e^{-b g_i^T D_1 g_i} + S_0 (1-f) e^{-b g_i^T D_2 g_i} \quad i = 1, 2, \ldots, N \qquad (4)$$

where S_i and S_0 are the signal intensities with and without diffusion weighting, f is a non-negative weight, g is the normalized gradient direction, b is the weighting factor, and D_1, D_2 are two tensors. Eq. (4) has 13 unknowns, compared to six in the single tensor case. The large number of parameters results in a high level of instability in estimating the tensors. The Levenberg-Marquardt nonlinear optimization algorithm was used to fit a mixture of Gaussian densities to the data. The initial step of our two-tensor estimation starts from using the least-squares single-tensor fit to the data by linear regression. The voxels were classified based on Westin measures [27] which determine the degree to which a tensor has linear (cl), planar (cp) or spherical (cs) shape. Two-tensor estimation was applied to planar voxels and single-tensor estimation to the other voxels, because only planar voxels are amenable to two tensor fitting.

Fibre Tractography: The two-tensor random-walk tracking method starts from a given seed point voxel. Every voxel in the data contains either 1 (single tensor) or 2 principal eigenvectors (two tensors) as appropriate for the tensor morphology of the particular voxel. If the seed voxel has two tensors then two separate trajectories are generated using two fibre orientations. A random-walk algorithm is then used to propagate the trajectories to the next position. If the next position contains two tensors, the corresponding two principle eigenvectors are compared to determine which of the trajectories (if any) should be followed. The diffusion tensor which has the most similar principal eigenvector to the principal eigenvector calculated from the previous position is chosen. The tracts are allowed to proceed along both positive and negative directions to obtain the full fibres. This process continues until the stopping criterion is met. The tractography algorithm describing these steps is given by Algorithm 1. This algorithm repeats for many random-walks (typically between 100 and 10000) and a region of interest, which contains a number of seed voxels.

Algorithm1: The two-tensor random-walk tractography algorithm.
1. Start from a given position x_0.
2. Compute the diffusion tensors D(x0) or D1(x0) and D2(x0) and corresponding major eigenvectors e(D(x0)) or e(D1(x0)) and $e(D_2(x_0))$ according to the tensor morphology of the position x_0.
3. The initial tracking step proceeds along both the positive and negative of these major eigenvectors directions from x_0 to obtain whole fibres (if x_0 is not a fibre endpoint).
4. If x_0 has two fibre directions then
   Generate two separate trajectories using.
   Trajectory 1: $v_0 = e(D_1(x_0))$
   Trajectory 2: $v_0 = e(D_2(x_0))$
   Else
   Generate one trajectory using $v_0 = e(D(x_0))$

Repeat
5. Obtain an updated position x_n ($1 \le n \le N$) using a random walk algorithm described in Table1.
6. If the position x_n contains two fibre directions
   Choose principal fibre direction at x_n as $e(D_c(x_n)) = e(D_1(x_n))$ or $e(D_2(x_n))$, so that the angular difference between the previous and current principal eigenvector ($v_{n-1}.e(D_i(x_n))$) is minimal.
   Else
   Choose principal fibre direction at x_n as $e(D(x_n))$
7. Compute v_n using a random walk algorithm de- scribed in Table1.
**Until** a stopping criterion is met

Synthetic Data Set: The two-tensor random-walk algorithms were validated in the presence of noise using two different simulated fibre geometries: two orthogonally crossing fibres with different values of FA for each fibre and a branching trajectory. The branching tract comprised an initial linear tract which diverged into two smoothly arching tracts. The single-tensor, two- tensor STE deterministic method and the two-tensor random-walk algorithm (Algorithm-E) were compared for

a range of SNRs. The appropriate parameter values were used from the optimization process for different SNRs.

Physical Phantom: The single-tensor random-walk (STRW) and two-tensor random-walk (TTRW) algorithms were applied to the physical phantom data, which simulates several complex pathway interactions, from 16 pre-defined seed positions with 1000 iterations. The results of our method were compared with that of the

(a)   (b)
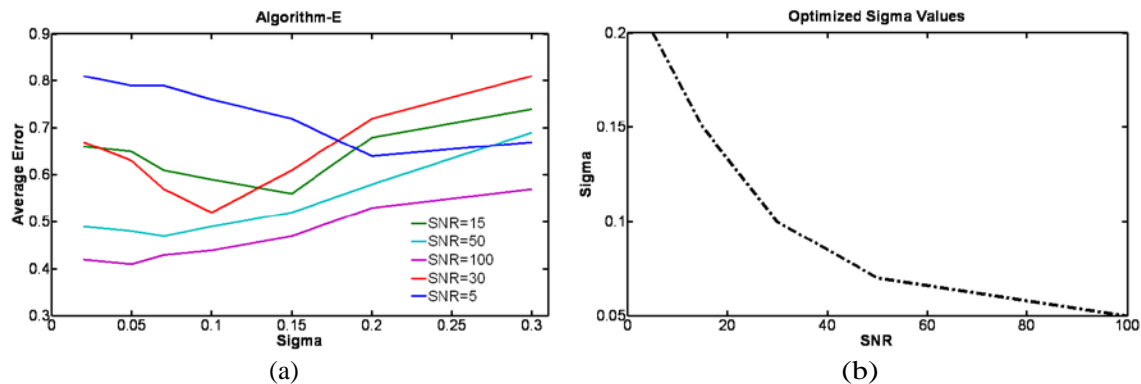
Fig. 1 (a) Plots of the average error (y-axis) as a function of σ (x-axis) for different SNR levels of the two synthetic datasets using Algorithm-E. (b) Optimized values of σ for different SNR levels.

(a)   (b)   (c)
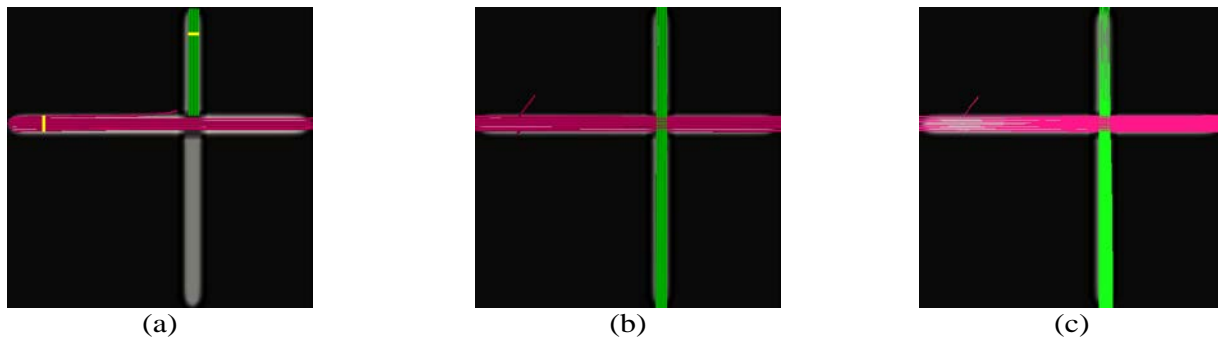
Fig. 2 Tracking results for two noise free orthogonal crossing fibre bundles using (a) STE, (b) two-tensor deterministic, and (c) two-tensor random-walk (Algorithm-E) algorithms. The reconstructed tracts are overlaid on the FA map.

(a)   (b)   (c)
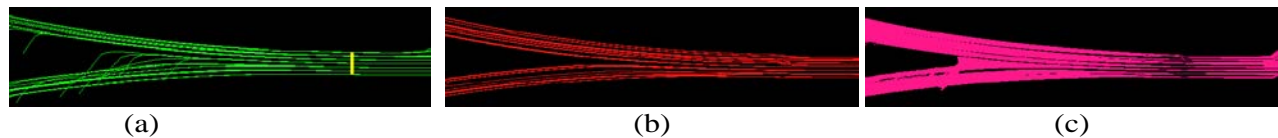
Fig. 3 Tracking results for two noise free branching fibre bundles using (a) STE, (b) two-tensor deterministic, and (c) two- tensor random-walk (Algorithm-E) algorithms.

STE [1] deterministic method applied to the same starting points as well as the ground truth.

***In Vivo* Data:** The performances of the STRW and TTRW algorithms in three different human data sets were examined within the centrum semiovale, where callosal tracts and corona radiata cross with longitudinal tracts. The tracking algorithms were seeded from two different seed points, one within the anterior body of the corpus callosum and the other lying in the left genu of the internal capsule. For comparison purposes, a parametric Bayesian method [8] and a non-parametric wild-bootstrapping method [5] were performed using the same seed points and the same stopping criteria.

The parameters used for phantom data and *in vivo* data were as follows: Algorithm-E ($\sigma = 0.1, \Delta t = 0.1$), Algorithm-T ($\sigma = 0.1, \Delta t = 0.1$) and Algorithm-TL ($\sigma = 0.1, \Delta t = 0.1, c_0 = 1/3, c_1 = 2/3$). The choice of σ and Δt values were based on the optimization process and visual inspection confirms that the values of c_0 and c_1 values are appropriate choices, especially in the complex regions. A constant curvature threshold (50^0) was used as stopping criterion for all cases.
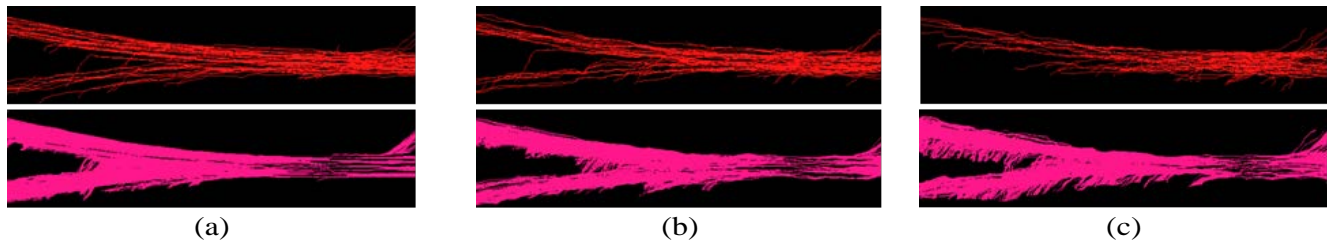
4. RESULTS

4.1 Synthetic Data Sets

Model Parameter Opti mization: Fig. 1(a) presents average error values for the 6 different seed points of the two synthetic data sets, as a function of σ (0.02 - 0.3) for different SNR levels (SNR= 5, 15, 30, 50 and 100). Generally the error first decreases

with σ and then

(a)   (b)   (c)
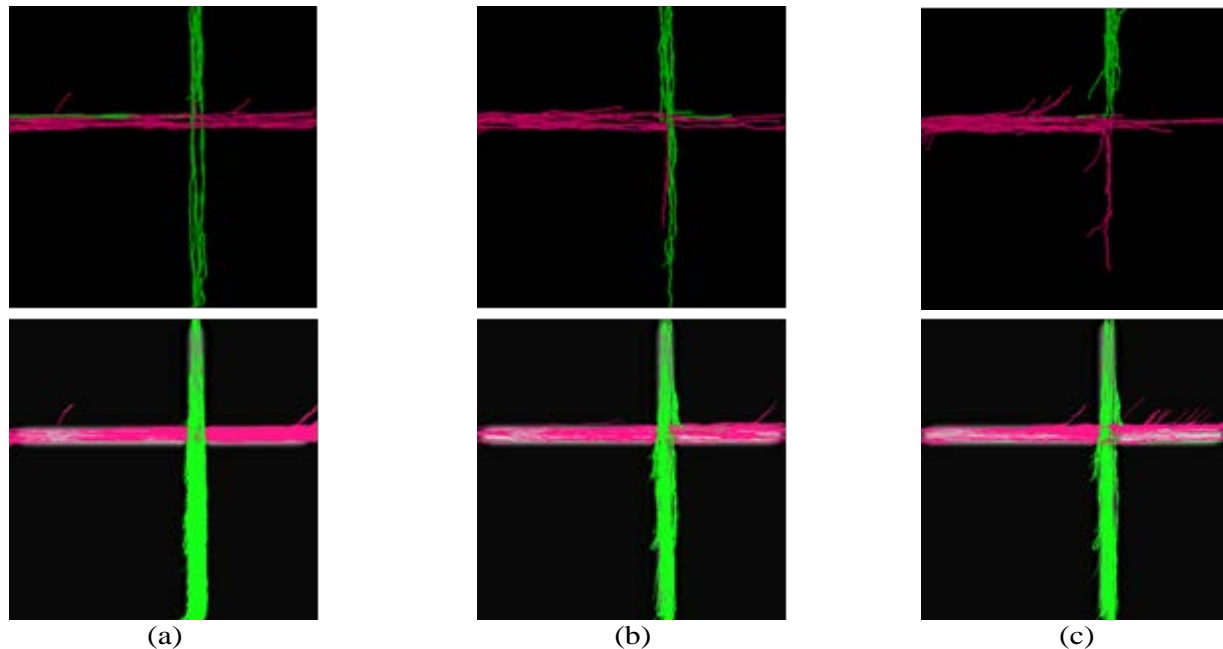
Fig. 4 The tracking results of the two-tensor deterministic (top row) and two-tensor random-walk (Algorithm-E) (bottom row) algorithms for two orthogonally crossing fibre bundles with SNRs of 30 (a), 15 (b) and 5 (c) respectively.


(a)   (b)   (c)

Fig. 5 The tracking results of the two-tensor deterministic (top row) and two-tensor random-walk (Algorithm-E) (bottom row) algorithms for branching fibre bundles with SNRs of 30 (a), 15 (b) and 5 (c) respectively.

later increases. The values of σ corresponding to the minimum average error values are considered as optimal for a particular SNR level (Fig. 1(b)). There was not   a large difference between the three algorithms in the optimized σ values. Some interesting simple relationships were observed in the step size optimization experiment. As might be expected, increasing the step size Δt (0.05 - 0.5 mm) in- creases the average error. This relationship was found to be approximately linear and independent of SNR, different fibre geometry or random-walk algorithm. This means that, in principle, it is possible to improve the quality of the tracking simply by reducing the step size.

Orthogonal Crossing Data: The orthogonal crossing data set contains two fibre bundles crossing at 90 degrees. Each tract has a different FA value. Fig. 2 shows the tracking results for noise free orthogonal crossing data. The ROIs for the evaluation are chosen at the start of the fibre bundles (coloured yellow in Fig. 2(a)).
Reconstructions of the horizontal fibre bundle with higher FA value are plotted in magenta; reconstructions originating in the second ROI on the vertical fibre bundle with lower FA are plotted in green. The tracking along the vertical path with the STE algorithm stops in the region of fibre crossing, as shown in Fig. 2(a). The eigenvector of the tensors in this region is dominated by the horizontal tract with higher FA. This dominance allows the horizontal reconstruction to continue undisturbed. If more than a single orientation per voxel is considered this problem is resolved, and the two crossing tracts are reconstructed correctly (Fig. 2(b) and (c)).
The performance of the TTRW algorithm was then tested for noisy data, as shown in Fig. 4. Tracking along the vertical and horizontal paths with a two-tensor deterministic method stops in the region of fibre crossing, especially in low SNR regions. The TTRW algorithm reconstructs both tracts completely and consistently.
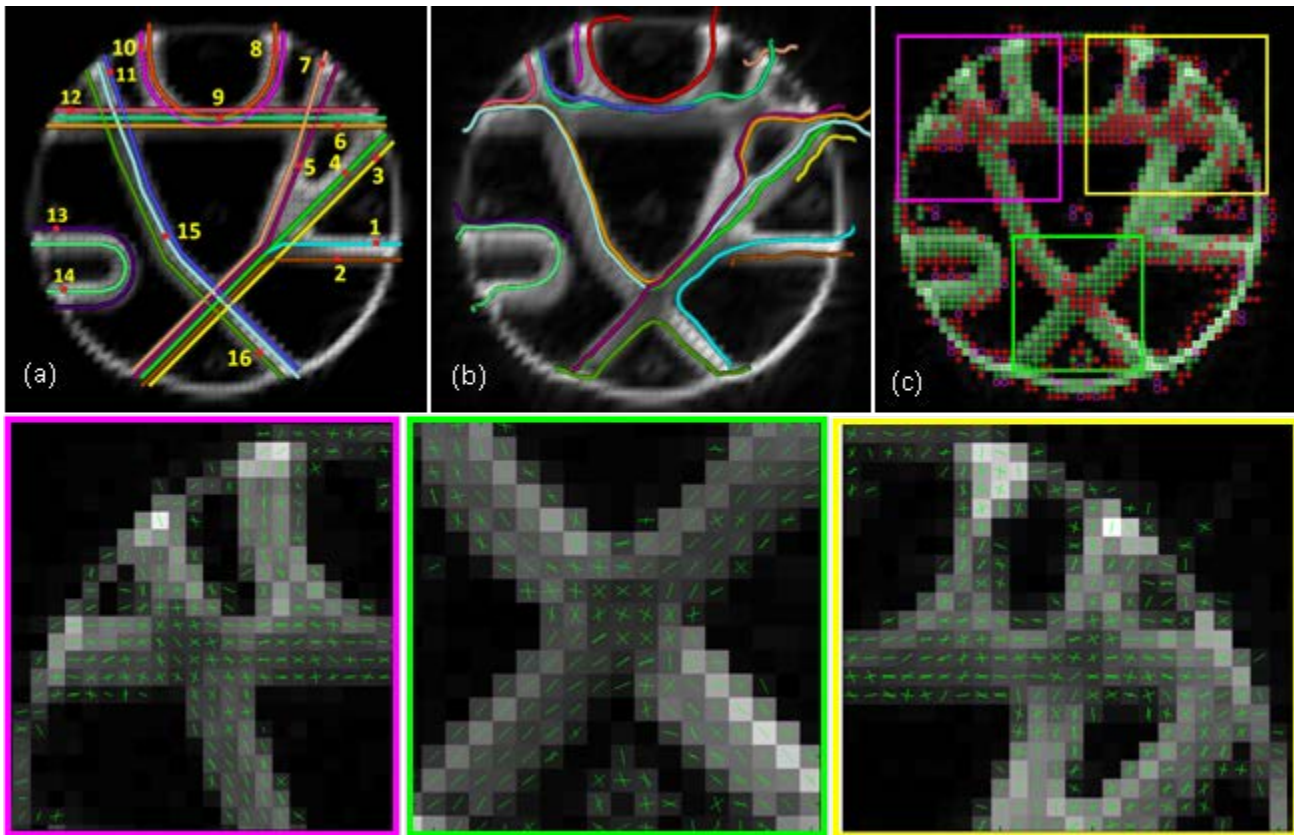
Fig. 6 Physical phantom (a) Ground truth and 16 seed points (b) STE deterministic tracking results (c) Westin measures (linear(+), planar(*) or spherical (o) shape) with three selected crossing regions and two-tensor estimation (bottom row).

Branching Data: The data set consists of two branching arms with each arm having a different FA value. The ROI was placed on the non-branching end of the fibre bundle (coloured yellow in Fig. 3(a)). Fig. 5 shows the reconstructed branching fibre bundle with two-tensor deterministic and two-tensor random-walk (Algorithm-E) algorithms. Many tracts of the deterministic results stop in the branching region and only reconstruct one arm completely, especially in low SNR data. However, the two-tensor random-walk algorithm reconstructs both arms completely in all cases.

These two examples clearly illustrate the advantages of the TTRW tracking methods in the noisy, crossing and branching fibre environments.

4.2 Phantom Data

The random-walk algorithms were evaluated on a physical phantom, which was created with the aim of bench- marking different tractography techniques [23]. Fig. 6(c) shows the Westin tensor morphologies [27] where the diffusion is disc-shaped, indicating the expected crossing fibre trajectories. A two-tensor model was fitted to voxels identified as planar and a single tensor model to the remaining voxels. The random-walk algorithms were applied to 16 pre-defined seed points for the physical phantom (Fig. 6(a)) using the single-tensor and two-tensor models. Fig. 7 shows the trajectories and the connectivity map from seed points 4, 9 and 14 using the three algorithms with a single-tensor model. Only some seed points results are shown to provide a clearer view. Algorithm-T identified longer tracts than Algorithm-E, and generated more smooth and stable tracts in comparison to Algorithm-E. Generally, the most probable paths from the particular seed points of all three algorithms are the same. To compare our method, the STE deterministic method was also applied using the same seed points. The STE trajectories (Fig. 6(b)) show un- usual tract behaviour, including sharp bends and loops.

The results of the STRW tracking are consistent with the ground truth except where some paths meet crossing regions. Fig. 8 shows the results of STRW tractography and TTRW tractography seeded through the area of identified fibre crossing using Algorithm-E. STRW fibre tractography results fail to pass through the crossing fibre area, where they stopped (Example: seed point 15) or leaked into unexpected regions and producing in- correct connections (Example: seed points 6, 5 and 1).
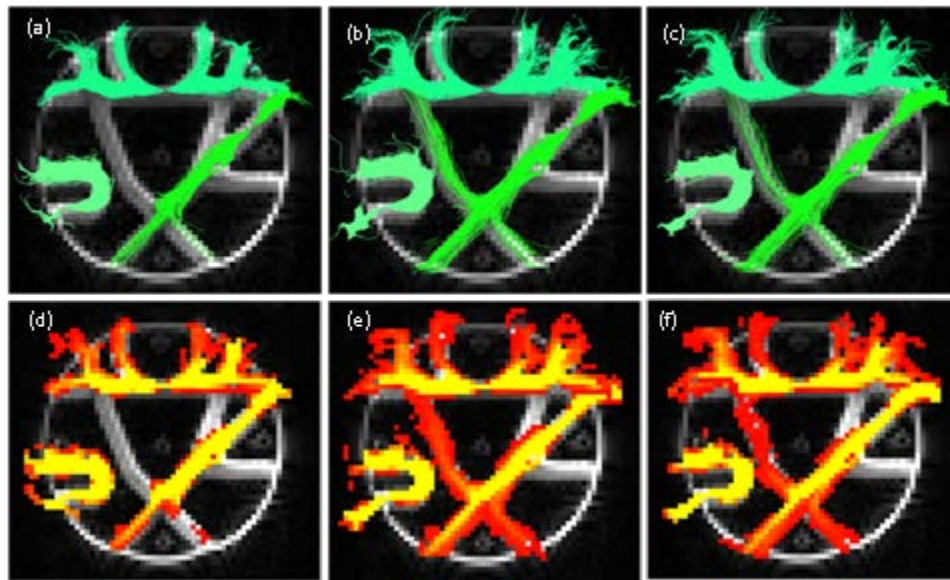
Fig. 7 Results of STRW tracking from seed points 4, 9 and 14 (a), (d) Algorithm-E (b),(e) Algorithm-T and (c),(f) Algorithm- TL
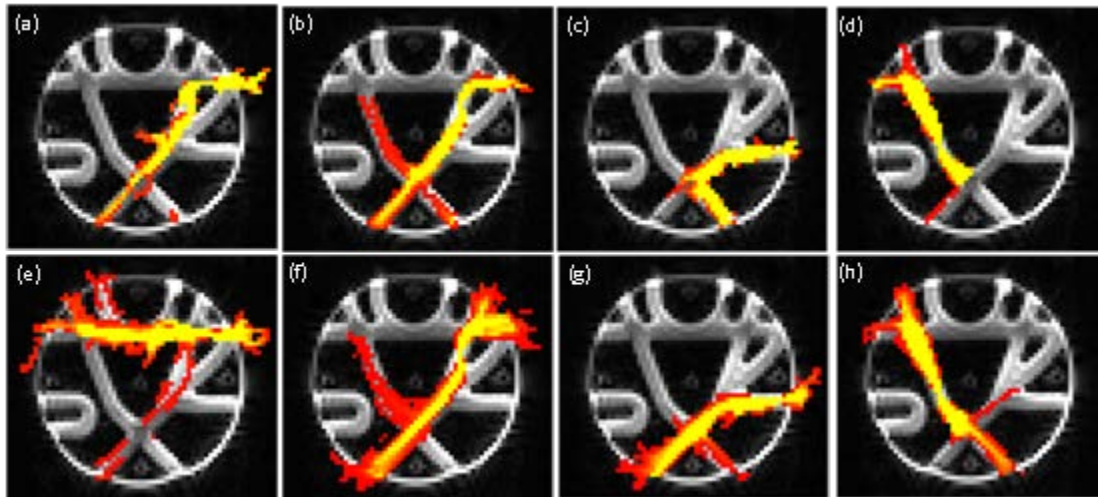
Fig. 8 Connectivity maps of STRW (top row) and TTRW (bottom row) algorithms using Algorithm-E from seed points (a),(b) 6 (c),(d) 5 (e),(f) 1 and (g),(h)15

The TTRW tracking results from these seed points are consistent with the ground truth.

These results show how our STRW tracking is able to give a clear output of fibre bundles from corresponding seed points in a way that is not possible with deterministic tracking. The proposed TTRW tracking approach performed better than the single-tensor approaches in the fibre crossing areas.

4.3 *In Vivo* Data

The majority of inter-hemispheric pathways are in the corpus callosum (CC), which has the highest anisotropy and moderate curvature. Fig. 9 shows typical results obtained from three healthy human subjects using the STRW tracking algorithms, TTRW tracking algorithms, Bayesian tracking method [8] and wild-bootstrapping method [5] for a seed point situated in the anterior body of the corpus callosum at the midline. The de- sired results observed from performing STRW tracking algorithms of the corpus callosum are its division into anatomic regions according to the fibre projections. The reconstructions obtained with the STRW tracking algorithms, Bayesian tracking method and wild bootstrap- ping are almost similar. However, tractography with these single-tensor methods estimates only medial tracts and were not able to resolve any crossing tracts. TTRW
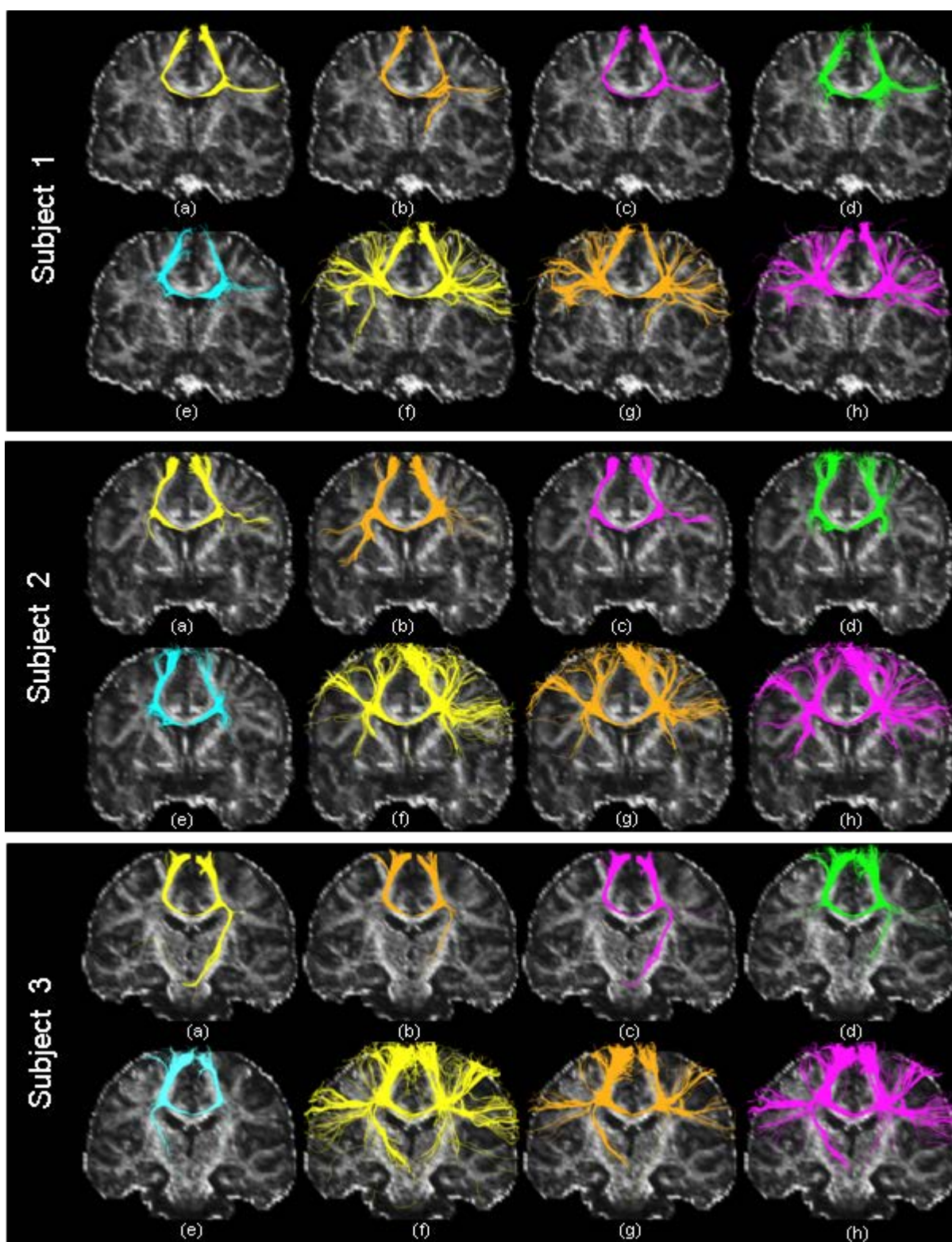
Fig. 9 Fibre tracking curves obtained using a seed point in the body of the corpus callosum for three different subjects and (a) STRW Algorithm-E (b) STRW Algorithm-T (c) STRW Algorithm-TL (d) Bayesian tracking (e) Wild-bootstrapping tracking (f) TTRW Algorithm-E (g) TTRW Algorithm-T (h) TTRW Algorithm-TL
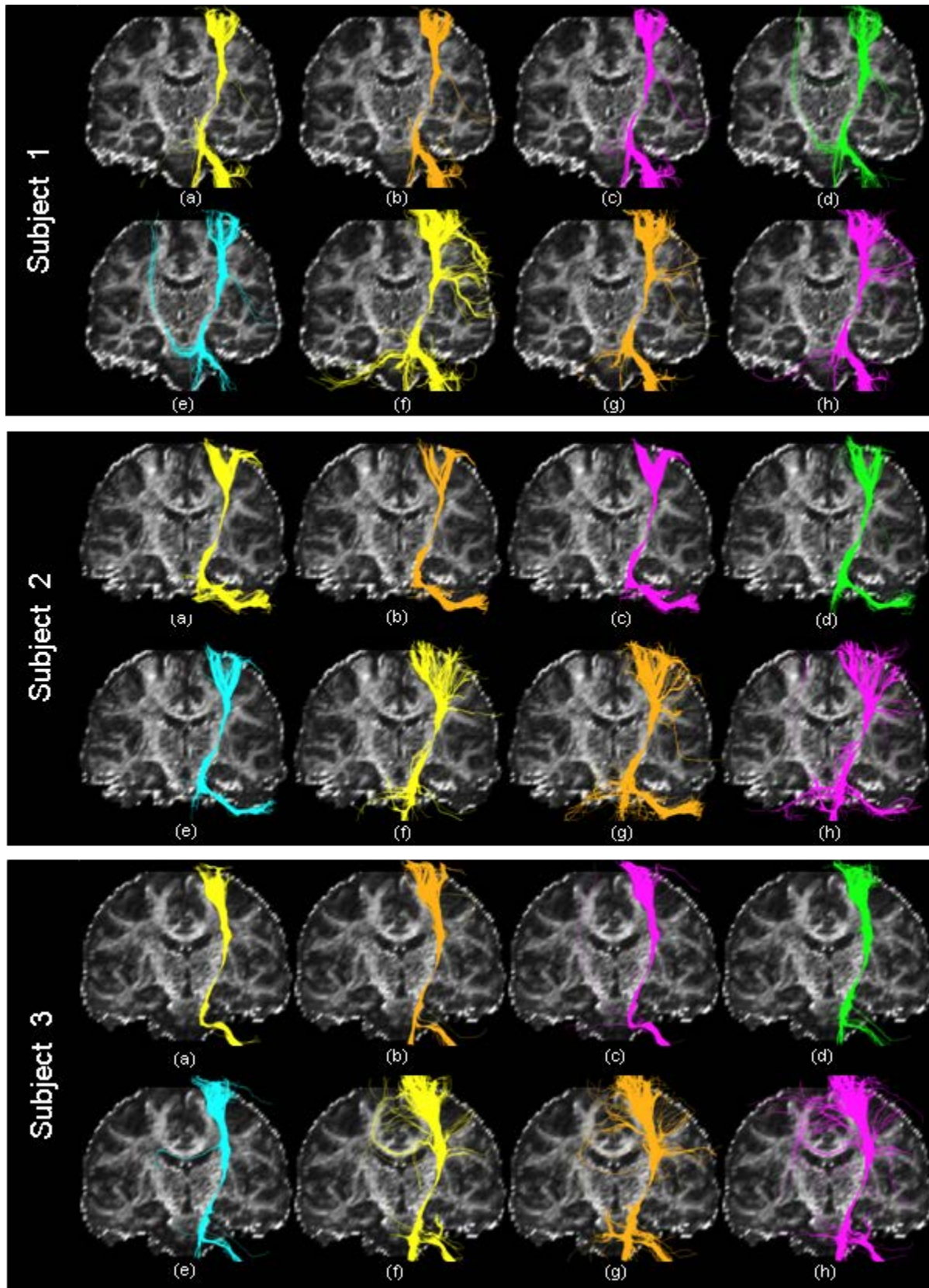
Fig. 10 Fibre tracking curves obtained using a seed point in the internal capsule for three different subjects and (a) STRW Algorithm-E (b) STRW Algorithm-T (c) STRW Algorithm-TL (d) Bayesian tracking (e) Wild-bootstrapping tracking (f) TTRW Algorithm-E (g) TTRW Algorithm-T (h) TTRW Algorithm-TL

tracking algorithms reconstructed a similar pattern of tracts across all subjects through the centrum semiovale and exhibited greater fanning of the callosal fibres to the cortex. Fibre paths for TTRW algorithms went through the crossing at the centrum

semiovale and the results capture lateral projections to the cortex. It should be pointed out that the results of TTRW algorithms (Fig. 9) were not perfectly symmetric in the two hemispheres for all three subjects.

The connections between the cerebral cortex and the spine, including the corticospinal tracts, are a part of the projection fibre system. Fig. 10 shows the results obtained from the seed point in the internal capsule using the STRW tracking algorithms, TTRW tracking algorithms, Bayesian tracking method [8] and wild- bootstrapping method [5]. The estimated corticospinal tracts of STRW tracking algorithms propagate inferiorly through the internal capsule and all the single- tensor tracking algorithms exhibit similar behaviour as the corpus callosum results. However, generally, these single-tensor tracking methods could not resolve the crossing between the corticospinal tract and the trans- verse pontine fibres. Tractography with TTRW how- ever exhibited greater fanning to the cortex compared to single-tensor approaches and was able to propagate to the different motor areas. TTRW performs better due to its ability to follow an appropriate, rather than any, fibre population in a crossing region.

The average computational time was estimated in each subject and compared with Bayesian tracking [8] and wild bootstrap tracking [5]. The computation time of the three tracking algorithms was defined in Fig. 9 as the time period required to yield a 3-D probabilistic path, beginning from the time that the *in vivo* diffusion weighted volumes were available. For the tracking experiments considered in Fig. 9, the average computation time (single processor) of our approach required less than 2 min, while the algorithms devised in [8] and [5] required >15 min and >10 min, respectively.

5. DISCUSSION

A number of probabilistic frameworks [4-8] have been proposed for fibre reconstruction as an alternative to deterministic streamline tractography, which has prob- lems in handling uncertainty in fibre orientations. Generally, these probabilistic techniques generate stream- lines in a Monte-Carlo fashion and define an index of connectivity using visitation maps. An important draw- back of these parametric and non-parametric probabilistic techniques is the computational time. Moreover, the repetitive streamline generation increases execution time, while the connectivity values can depend on the total number of streamlines launched.

In this study, simple and computationally efficient random-walk probabilistic fibre tracking algorithms, building on the basic deterministic methods [1-3], have been presented for estimating uncertainty in fibre orientation and anatomical connectivity in white matter. How- ever, complex fibre configurations cannot be resolved by a conventional single-tensor model. These algorithms are therefore applied to a two-tensor model where the voxels are classified based on tensor morphologies be- fore applying a single or two-tensor model. Synthetic data results showed that the two-tensor random-walk approach was successful in resolving the crossing and branching regions, particularly in cases of low SNR. Physical phantom and *in vivo* tractography results further supported these findings and showed the improved computational efficiency compared to conventional probabilistic approaches.

The principal eigenvector direction of DTI may not reflect actual fibre directions in noisy data and can be undefined in crossing regions. Random-walk algorithms are therefore developed here, which take into account more characteristics of the tensor field than only the directions of the principal eigenvectors. Despite using a simple model, it has been demonstrated how uncertainty can be taken into account during the tracking procedure. Using a random-walk approach, the tracking procedure has been extended from one-to-one mapping to a one-to-many mapping. This could give a better view of connectivity in the brain, taking branching of fibres into account.

STRW tracking results were compared against the results of two conventional parametric [8] and non para- metric [5] tractography algorithms using three human subjects. The results of STRW algorithms confirm the effectiveness of the proposed approach, which gives com- parable results to other probabilistic methods. The probabilistic random-walk algorithms are however fast, re- quire less memory and are relatively easy to implement. The computational cost of the algorithms can vary widely, depending on the resolution of the data set, step size and stopping criteria, seed point and the algorithm parameters supplied by the user. However, from our experiments on real data the random-walk algorithms are significantly quicker than the time to generate all possible tracts using other probabilistic methods from a seed point. The STRW tracking algorithms show promise in resolving the problems of deterministic tracking methods and the standard probabilistic methods.

The key parameters in these algorithms are the step size Δt and noise ratio σ. Generally, these parameters influence the results of the random-walk fibre tracking algorithms. Here we used optimal tuning of these parameters based on the use of simulated data with a range of SNRs. We used synthetic data to analyze the random-walk models quantitatively and thereby estimated the optimal parameter values of the models. We performed the STRW tracking method on straight and branching geometrical shapes for optimization since we optimized the parameters against noise only and the results of single-tensor tracking algorithms are most likely to be affected by crossing fibres. It may be sensible to use the STE algorithm for highly prolate tensor voxels and to use the TEND algorithm when the diffusion tensor has a more oblate or spherical tensor shape [2]. The user defined weighting factors c_0 and c_1 in the Algorithm-TL dynamically adjust these tensor morphologies circumstances. The performance of the tracking algorithms has been verified using these optimal parameter values and a physical phantom and an *in vivo* datasets with a wide variety of seed points. Our results show that, in general, tracking with high SNR and a low step size gives the most reliable results.

Hagmann et al. [8] proposed a random walk model of a particle diffusing in a diffusion tensor field to assess uncertainty in tractography. They provided many parameters (η, α and λ) in their random-walk algorithm, however, there was no

experiments presented for optimal tuning the parameters. One of the main disadvantages of this method is that there is no deterministic limit of the algorithm: when the stochastic part of the algorithm vanishes ($\lambda = 0$), a track turns into a straight line ($\Omega_i = \Omega_{i-1}$) compared with our algorithms which perform in a basic deterministic way when $\alpha = 0$.

An important drawback of the conventional diffusion tensor model is its limited ability to present de- tailed information about multidirectional fibre architecture within a voxel. We therefore further extended these algorithms to a two-tensor model for resolving crossing fibre configurations, a major concern in DW imaging, using data that can be routinely acquired in a clinical setting. Two-tensor estimation was performed only on planar voxels by classifying the morphology of the tensor. A model selection procedure was necessary to identify regions where DTI fails. Planarity was quantified using the planar index cp [27]. In planar regions, an oblate DTI tensor was decomposed into multiple compartments with orientations compatible with the neighbourhood. The recent super-resolved spherical de- convolution method [28] has shown satisfactory results in resolving fibre crossings using DTI data acquired in 4.5 minutes, however, only orientational estimates are given by this technique. PASMRI [18] has also shown good results using relatively low angular resolution DTI data, however it has very high computational requirements.

Using simulated datasets we demonstrated the performance of the two-tensor random-walk algorithms for different SNR levels. We successfully applied this method for the extraction of the callosal fibres and corticospinal tracts from *in vivo* data. The *in vivo* example showed the ability of the algorithms to resolve crossing regions, but also demonstrates the limitations of this DTI-based approach. We have illustrated the results using a single seed point in order to provide a clear view of multiple random-walk patterns and to simplify the evaluation. Finally, the robustness and the reproducibility of the method confirmed experimentally using 3 human brain datasets.

The random-walk probabilistic approach presented here is governed by the assumption that a maximum number of two crossing tracts can be resolved. In cases of three crossing populations the DTI diffusion profile will be mostly spherical and in such cases could be identified using Westins spherical index cs [27] within white matter and a three-tensor model fitted. Reducing the step size Δt could improve accuracy but since decreasing the step size increased computational time slightly, so 0.1 was considered a good compromise between ac- curacy and speed.

6. CONCLUSION

Simple and computationally efficient random-walk probabilistic algorithms have been presented, motivated by the fact that deterministic tracking algorithms have difficulties handling regions of low anisotropy and noise. For resolving fibre crossings using DW-MRI data, multi-tensor random-walk algorithms were developed and crossing orientations were estimated utilizing two-tensor models, applied to voxels with a planar diffusion profile. Tractography results were improved using the appropriate estimates of the model parameters from an optimization scheme. Based on our experimental evaluations, unlike previous standard probabilistic methods which are computationally very expensive, our algorithms can accurately reconstruct fibre paths with substantially improved computational efficiency as com- pared to conventional methods. The ability of multi- tensor random-walk algorithms to reconstruct complex intra-voxel structures robustly and rapidly is of relevance to both in research and clinical applications.

REFERENCES

[1] Basser PJ, Pajevic S, Pierpaoli C, Duda J, Aldroubi A (2000) In vivo fiber tractography using DT-MRI data. Magn. Reson. Med. 44:625-632

[2] Lazar M, Weinstein DM, Tsuruda JS, Hasan KM, Arfanakis K, Meyerand ME, Badie B, Rowley HA, Haughton V, Field A, Alexander LA (2003) White matter tractography using diffusion tensor deflection. Hum. Brain Mapp. 18:306-321

[3] Weinstein D, Kindlmann G, Lundberg E (1999) Tensorlines advection-diffusion based propagation through diffusion tensor fields. In: IEEE visualization conference, San Francisco, CA, p 249-253

[4] Lazar M, Alexander A (2005) Bootstrap white matter tractography (BOOT-TRAC). NeuroImage 24(2):524-532

[5] Jones DK (2008) Tractography gone wild: probabilistic fibre tracking using the wild bootstrap with diffusion tensor MRI. IEEE Trans. Med. Imaging 27:1268-1274

[6] Chung S, Lu Y, Henry RG (2006) Comparison of boot- strap approaches for estimation of uncertainties of DTI parameters. NeuroImage, 33:531-541

[7] Behrens TEJ, Woolrich MW, Jenkinson M (2003) Characterization and propagation of uncertainty in diffusion-weighted MR imaging, Magn. Reson. Med. 50(5): 1077- 1088

[8] Friman O, Farnback G, Westin CF (2006) A Bayesian approach for stochastic white matter tractography. IEEE Trans. Med. Imaging 25(8):965-978

[9] Lazar M, Alexander AL (2002)White matter tractography using random vector (RAVE) perturbation. In: 10th Annual Meeting ISMRM, Honolulu, HI, USA, p 539

[10] Prigarin, SM, Hahn K (2005) Stochastic algorithms for white matter fiber tracking and the inference of brain connectivity from MR diffusion tensor data. In:Sonderforschungsbereich 386, p 408

[11] Hagmann P, Thiran JP, Jonasson L, Vandergheynst P, Clarke S, Maeder P, Meuli R (2003) DTI mapping of human brain connectivity: statistical fibre tracking and virtual dissection. NeuroImage 19(3):545-554

[12] Ratnarajah N, Simmons A, Davydov O, Hojjatoleslami A (2010) A novel white matter fibre tracking algorithm using probabilistic tractography and average curves. In: MICCAI 13:666-73

[13] Alexander AL, Hasan KM, Lazar JS, Parker DL (2001) Analysis of partial volume effects in diffusion-tensor MRI. Magn. Reson. Med. 45:770-780

[14] Tuch DS, Reese TG, Wiegell MR, Makris N, Belliveau JW, Wedeen VJ (2002) High angular resolution diffusion imaging reveals intravoxel white matter fiber het- erogeneity. Magn. Reson. Med. 48(4):577-82

[15] Tuch DS (2004) Q-ball imaging. Magn. Reson. Med. 52:1358-1372

[16] Wedeen VJ, Hagmann P, Tseng WY, Reese TG, Weisskoff RM (2005) Mapping complex tissue architecture with diffusion spectrum magnetic resonance imaging. Magn. Reson. Med. 54:1377-86

[17] Tournier JD, Calamante F, Gadian DG, Connelly A (2004) Direct estimation of the fiber orientation density function from diffusion-weighted MRI data using spherical deconvolution. Neuroimage 23:1176-85

[18] Jansons KM, Alexander DC (2003) Persistent angular structure: new insights from diffusion magnetic resonance imaging data. Inverse Probl. 19:1031-46

[19] Behrens TEJ, Johansen-Berg H, Jbabdi S, Rushworth MFS, Woolrich MW (2007) Probabilistic diffusion tractography with multiple fibre orientations. What can we gain? NeuroImage 34(1):144-155

[20] Berman JI, Chung S, Mukherjee CP, Han ET, Henry RG (2008) Probabilistic streamline q-ball tractography using the residual bootstrap. NeuroImage 39(1):215-222

[21] Ratnarajah N, Simmons A, Colchester A, Hojjatoleslami A (2011) Resolving complex fibre configurations using two-tensor random-walk stochastic algorithms. In: SPIE Medical Imaging 7962-26(OR)

[22] Deoni SCL, Jones DK (2005) Generation of a common diffusion tensor imaging dataset. In: ISMRM workshop on methods for quantitative diffusion MRI of human brain.

[23] Poupon C, Rieul B, Kezele I, Perrin M, Poupon F, Mangin JF (2008) New diffusion phantoms dedicated to the study and validation of high-angular-resolution diffusion imaging (HARDI) models. Magn. Reson. Med. 60(6):1276-83

[24] Smith SM, Jenkinson M, Woolrich MW, Beckmann CF, Behrens TE, Johansen- Berg H, Bannister PR, De Luca M, Drobnjak I, Flitney DE, Niazy RK, Saunders J, Vickers J, Zhang Y, De Stefano N, Brady JM, Matthews PM (2004) Advances in functional and structural MR image analysis and implementation as FSL. Neuroimage 23 Suppl 1:S208-19

[25] Woods RP, Grafton ST, Holmes CJ, Cherry SR, Mazziotta JC (1998) Automated image registration: I. General methods and intrasubject, intramodality validation. J. Comput. Assist. Tomo. 22:139-152

[26] Kingsley PB (2006) Introduction to diffusion tensor imaging mathematics, Part I. Tensors, rotations, and eigenvectors. Concept. Magnetic. Res. Part A 28A:101- 122

[27] Westin CF, Maier SE, Mamata H, Nabavi A, Jolesz FA, Kikinis R (2002) Processing and visualization for diffusion tensor MRI. Med. Image Anal. 6:93-108.

[28] Tournier JD, Calamante F, Connelly A 2007 Robust de- termination of the fibre orientation distribution in diffusion MRI: non-negativity constrained super-resolved spherical deconvolution. Neuroimage 35:1459-72

AUTHORS

First Author – Jeyarasa Pratheepan, BSc (Hons) MSc (Computer Science), Sri Lanka Institute of Advanced Technological Education (SLIATE), jpt.cbc@gmail.com.

Second Author – Niroji Thayalan, BSc in Computer Science and Technology, Sri Lanka Institute of Advanced Technological Education (SLIATE), nirojiuwucst@gmail.com.

Correspondence Author – Jeyarasa Pratheepan, jpt.cbc@gmail.com, +94773659589.